

## Evolution of tachyon kink with electric field

---

### Inyong Cho

*Department of Physics and BK21 Physics Research Division  
Sungkyunkwan University, Suwon 440-746, Korea  
E-mail: iycho@skku.edu*

### O-Kab Kwon

*Center for Quantum Spacetime  
Sogang University, Seoul 121-742, Korea  
E-mail: okabkwon@sogang.ac.kr*

### Chong Oh Lee

*Department of Physics, Chonbuk National University  
Chonju 561-756, Korea  
E-mail: cohlee@chonbuk.ac.kr*

**ABSTRACT:** We investigate the decay of an inhomogeneous D1-brane wrapped on a  $S^1$  with an electric field. The model that we consider consists of an array of tachyon kink and anti-kink with a constant electric flux. Beginning with an initially static configuration, we numerically evolve the tachyon field with some perturbations under a fixed boundary condition at diametrically opposite points on the circle  $S^1$ . When the electric flux is smaller than the critical value, the tachyon kink becomes unstable; the tachyon field rolls down the potential, and the lower dimensional D0- and  $\bar{D}0$ -brane become thin, which resembles the caustic formation known for this type of the system in the literature. For the supercritical values of the electric flux, the tachyon kink remains stable.

**KEYWORDS:** Tachyon Condensation, D-branes.

---

## Contents

<b>1. Introduction</b>	<b>1</b>
<b>2. Dp-brane model with tachyon and electric field</b>	<b>2</b>
<b>3. Evolution of tachyon kink array on D1-brane</b>	<b>4</b>
3.1 Pure tachyon case ( $\Pi = 0$ )	6
3.2 Tachyon with electric flux ( $\Pi \neq 0$ )	8
3.2.1 Unstable solution	8
3.2.2 Stable solution	12
<b>4. Semi-analytic approach</b>	<b>15</b>
4.1 Pure tachyon case ( $\Pi = 0$ )	16
4.2 Tachyon with electric flux ( $\Pi \neq 0$ )	16
4.3 Caustic formation revisited	17
<b>5. Conclusions</b>	<b>18</b>

---

## 1. Introduction

Spatially inhomogeneous rolling tachyon on an unstable D-brane has been studied in boundary conformal field theory (BCFT) [1–3], boundary string field theory (BSFT) [4], and Dirac-Born-Infeld (DBI)-type effective field theory [5–15]. In BCFT, this subject was considered in the presence of spacetime-dependent marginally deformed tachyon vertex operator at the worldsheet boundary. The evolution of the resulting energy-momentum tensor is qualitatively different from that of the homogeneous rolling tachyon [16, 17]. The energy density evolves into a localized delta-function array within a finite critical time. These delta-function singularities were interpreted as codimension-one D-branes [1–3].

In lower-energy effective field theory approaches for unstable D-branes, most of the actions involve only the first derivatives of fields on the brane. Since the actions are represented by truncating all the higher derivatives of fields, they are considered reliable only when the second and higher derivatives are small. Nonetheless, the effective actions have been shown to reproduce various nontrivial aspects of the unstable D-brane dynamics in special settings, for example, the spatially homogeneous rolling tachyon [18–21] and lower dimensional D-branes as static worldvolume solitons [22–28].

In an inhomogeneous time evolution of an unstable D-brane, however, its dynamics is not governed by a truncated effective action after a certain critical time. Felder et. al. showed that caustics develop in some regions during the evolution of the inhomogeneous

tachyon field with a runaway potential in the DBI-type action [5]. They treated the tachyon as a collisionless fluid and found that the tachyon field becomes multi-valued in those regions within a finite critical time. They interpreted the caustics as a signal that the higher derivatives of the tachyon field blow up [5, 11]. More examples for the pure tachyon evolution have been investigated in refs. [6, 8]. They observed that the slope of the tachyon field near the kink diverges within a finite time. Authors identified this phenomenon with the caustic formation observed in ref. [5].

Interesting aspects of the low energy effective field theory with an electric flux turned on, have been considered in the tachyon vacuum [29, 20, 21, 30, 31, 15]. In this work, we shall examine the role of the electromagnetic fields on an unstable D-brane where those fields are varying in time and in space with a nonzero flux. The electric flux density here is identified with the string charge density on the D-brane [32, 33]. When the tachyon and the electromagnetic fields depend on time (or one spatial) coordinate only, the equations of motion imply that all the electromagnetic fields are constants [21, 25]. Consequently, the electromagnetic fields become simply parameters of the tachyon solution. However, in an inhomogeneous time evolution process, the electromagnetic fields depend on both time and space in general [15].

In this paper, we shall consider a simple case in the DBI-type action which contains a tachyon and a single electric field. The electric field is turned on along the inhomogeneous direction which we restrict to be a circle  $S^1$ . Assuming that the tachyon and the electric field depend on time and one spatial coordinate, we numerically solve the master equation of the tachyon field under a fixed boundary condition at diametrically opposite points, which is closely related to the formation of the D0- $\bar{D}0$  pair located at diametrically opposite points on the circle  $S^1$  [34–36].

We find that there exists a critical value of the string charge density under which the kink is unstable. The kink approaches a similar state which resembles the caustic formation observed in the pure tachyon case [8]. If the string charge density is increased above the critical value, we find that the tachyon kink becomes stable.

In section 2, we present the  $Dp$ -brane model with a tachyon and an electric field in the DBI-type action. In section 3, we numerically solve the field equation and discuss the stability. In section 4, we analyze the stability in a semi-analytic manner, and conclude in section 5.

## 2. $Dp$ -brane model with tachyon and electric field

We shall consider the dynamics of the tachyon field described by DBI-type action in the presence of gauge field interactions. With general gauge field interactions, the tachyon and the gauge fields are coupled in a very complicated manner. Therefore, we shall consider the simplest case in which the tachyon field depends on time and on one spatial coordinate only while the electric field is turned on along that inhomogeneous spatial direction.

The DBI-type action with gauge field interactions on an unstable  $Dp$ -brane in flat

space is given by [37–39]

$$S = -\mathcal{T}_p \int d^{p+1}x V(T)\sqrt{-X}, \quad (2.1)$$

$$X = \det(\eta_{\mu\nu} + \partial_\mu T \partial_\nu T + F_{\mu\nu}), \quad (\mu, \nu = 0, 1, \dots, p), \quad (2.2)$$

where  $\mathcal{T}_p$  is the unstable  $Dp$ -brane tension,  $V(T)$  is a runaway tachyon potential, and  $F_{\mu\nu}$  is the field-strength tensor for the gauge field  $A_\mu$ . The equations of motion for the tachyon and the gauge field read

$$\partial_\mu \left( \frac{VC_S^{\mu\nu}}{\sqrt{-X}} \partial_\nu T \right) + \sqrt{-X} \frac{dV}{dT} = 0, \quad (2.3)$$

$$\partial_\mu \left( \frac{VC_A^{\mu\nu}}{\sqrt{-X}} \right) = 0, \quad (2.4)$$

where  $C_{S(A)}^{\mu\nu}$  is the symmetric (anti-symmetric) part of the cofactor for the matrix  $(\eta + \partial T \partial T + F)_{\mu\nu}$ . We consider the tachyon and the electric field along the inhomogeneous direction living in the worldvolume of the  $Dp$ -brane,

$$T = T(x^0, x^1), \quad E \equiv F_{01}(x^0, x^1), \quad (2.5)$$

and, for simplicity, turn off all the other components of the electromagnetic field. For the unstable D1-brane, the above field ansätze (2.5) are the general setting with no restriction. With these fields on the unstable  $Dp$ -brane, the quantity  $X$  and the cofactor matrix are simplified as

$$X = -(1 - \dot{T}^2 + T'^2 - E^2), \quad (2.6)$$

$$(C^{\mu\nu}) = \begin{pmatrix} 1 + T'^2 & E - \dot{T}T' \\ -E - \dot{T}T' & -1 + \dot{T}^2 \end{pmatrix}, \quad (2.7)$$

where  $\dot{T} \equiv \partial_0 T$ ,  $T' \equiv \partial_1 T$  and all other components of  $C^{\mu\nu}$  are trivial, i.e.,  $C^{\mu\nu} = \delta^{\mu\nu}$ .

The solution to the gauge field equation (2.4) is then simply

$$\Pi \equiv \beta E = \text{constant}, \quad (2.8)$$

where  $\Pi \equiv \partial \mathcal{L} / \partial (\partial_0 A_1) = \partial \mathcal{L} / \partial E$  is the conjugate momentum for the gauge field  $A_1$  in the Weyl gauge  $A_0 = 0$ . We also have a defined quantity

$$\beta \equiv \frac{\mathcal{T}_p V}{\sqrt{-X}}. \quad (2.9)$$

Using eq. (2.8), we can express the electric field  $E$  with the tachyon field  $T$  and the constant electric flux  $\Pi$  as

$$E^2 = \frac{\Pi^2(1 - \dot{T}^2 + T'^2)}{\Pi^2 + \mathcal{T}_p^2 V^2}. \quad (2.10)$$

The tachyon field equation (2.3) which completely governs the dynamics of the unstable D-brane, is now written as

$$(1 + T'^2)\ddot{T} - (1 - \dot{T}^2)T'' - 2\dot{T}T'\dot{T}' + \frac{\mathcal{T}_p^2 V(1 - \dot{T}^2 + T'^2)}{\Pi^2 + \mathcal{T}_p^2 V^2} \frac{dV}{dT} = 0. \quad (2.11)$$

Setting  $\Pi = 0$  in the above equation (2.11), we obtain the field equation for the pure tachyon [5].

The components of the energy-momentum tensor are

$$T^{00} = \beta(1 + T'^2) \quad (2.12)$$

$$T^{01} = -\beta\dot{T}T', \quad (2.13)$$

$$T^{11} = -\beta(1 - \dot{T}^2). \quad (2.14)$$

Before we close this section, let us comment on what was studied for the pure tachyon case ( $\Pi = 0$ ) in a relation to a caustic formation. It is well-known that the tachyon potential for large  $T$  exponentially decays,  $V(T) \sim e^{-\alpha T}$  with an arbitrary positive constant  $\alpha$  [18]. Then for the case of pure tachyon field ( $\Pi = 0$ ), the tachyon equation (2.11) is reduced to [5]

$$(1 + T'^2)\ddot{T} - (1 - \dot{T}^2)T'' - 2\dot{T}T'\dot{T}' = \alpha(1 - \dot{T}^2 + T'^2). \quad (2.15)$$

It was shown in the literature [5, 8, 9, 11] that eq. (2.15) develops a caustic at a finite time, which we shall reconsider in section 4.3.

On the other hand, with a nonvanishing electric flux  $\Pi$ , eq. (2.11) is rewritten as

$$(1 + T'^2)\ddot{T} - (1 - \dot{T}^2)T'' - 2\dot{T}T'\dot{T}' = -B(T)(1 - \dot{T}^2 + T'^2), \quad (2.16)$$

where

$$B(T) = \frac{\mathcal{T}_p^2 V}{\Pi^2 + \mathcal{T}_p^2 V^2} \frac{dV}{dT}. \quad (2.17)$$

We shall discuss the role of the electric flux  $\Pi$  for the 1/cosh-type tachyon potential in section 4 by investigating the behaviors of  $B(T)$  for various  $\Pi$ 's.

### 3. Evolution of tachyon kink array on D1-brane

In this section we investigate the time evolution of an inhomogeneous tachyon kink array on an unstable D1-brane in the presence of an electric field. The D1-brane now contains a fundamental string with a string charge density  $\Pi$ . We shall also discuss the subsequent dynamical formation of the lower dimensional D0/ $\bar{D}0$ -brane. Although we focus on the D1-brane for simplicity, the results are generally applied to  $Dp$ -branes when only one spatial direction of them is inhomogeneous. We solve the time-dependent field equation (2.11) numerically with a well-known tachyon potential

$$V(T) = \frac{1}{\cosh\left(\frac{T}{\sqrt{2}}\right)}. \quad (3.1)$$

For the constant electric field,  $E = E_0$ , with the above potential the static regular kink solution was obtained in ref. [25]. For  $0 < E_0^2 < 1$ , the solution reads

$$T_0(x) = \sqrt{2} \sinh^{-1} \left[ \sqrt{\frac{\mathcal{T}_1^2}{\beta_0^2 - \Pi^2} - 1} \sin \left( \frac{\sqrt{\beta_0^2 - \Pi^2}}{\sqrt{2}\beta_0} x \right) \right], \quad (3.2)$$

where the constant  $\beta_0 = \Pi/E_0$  is the value of  $\beta$  for the static solution. This solution represents a tachyon kink-anti-kink array on a D1-brane, and reduces to a *pure* tachyon solution when  $\Pi = 0$  [23].

In order to investigate the tachyon evolution, we evolve this static solution with a “minimal” perturbation by solving the time-dependent field equation (2.11). Here, the minimal perturbation is implied by imposing the initial conditions,

$$T(t = 0, x) = T_0(x), \quad (3.3)$$

$$\dot{T}(t = 0, x) = 0. \quad (3.4)$$

In principle, if the the initial velocity of the tachyon field is zero, the system never evolves; it is easy to see from the field equation (2.11) that the static solution remains as the solution in the course of evolution. However, in numerical simulations, the intrinsic numerical errors coming from the numerical scheme play a role of perturbation. Once the numerical code is stable, the tiny numerical error induces a minimal perturbation to the static system. If the initial configuration is physically stable, the system will not evolve except exhibiting small fluctuations. On the other hand, if the system evolves from the initial configuration as time elapses, it means that the system is physically unstable. This is not from the numerical instability. Therefore, applying such a minimal perturbation is very useful for a system at present which is suspected unstable to form a caustic at later times.

The boundary condition we impose is

$$T(t, x_n) = 0, \quad (3.5)$$

where  $x_n$  is the location of the  $n$ -th node of the initial static configuration (3.2). This boundary condition implies that we fix the spatial coordinates of the kink/anti-kink centers during evolution. By doing so, we may consider the time evolution of only one patch (a half period) of the kink array, and the rests are merely a duplication of that patch configuration. Under the boundary condition (3.22), the compactification radius is fixed by the periodicity of the static kink solution while it was not fixed in the Sen’s work in ref. [35].

The initial conditions, (3.3) and (3.4), imply the “point symmetry” about the kinks and the “reflection symmetry” about the line  $x = x_{\max}$  where the tachyon field has the maximum value. The boundary condition (3.5) that we impose preserves such symmetries in the course of evolution. For the pure tachyon case, we can observe the formation of the D0- $\bar{D}0$  pair located at diametrically opposite points on the circle  $S^1$  initiated by Sen, and with the given boundary condition the  $Z_2$  symmetry is preserved [34–36]. In the presence of electric flux, we impose the boundary condition in the same way as we do for the pure tachyon case, although the  $Z_2$  symmetry is now absent; we believe that it is an appropriate and the simplest set-up that we can consider in the first step for the stability check.

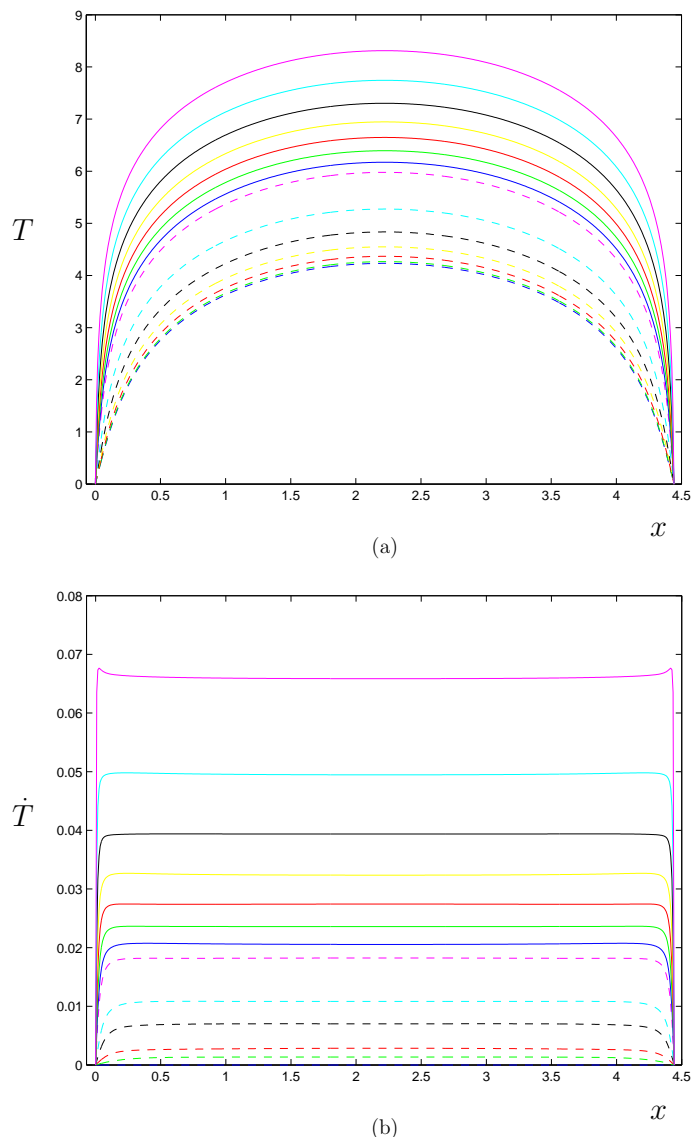


**Figure 1:** Plot of (a)  $T(t, x)$  and (b)  $\dot{T}(t, x)$  for the pure tachyon case with  $\beta_0^2 = 10^{-2}\mathcal{T}_1^2$ . From the bottom, the lines correspond to  $t = 0, 50, 100, \dots, 300, 310, 320, \dots, 370$ . (The line style and color are in the same order in the rest of figures.) In (a), the tachyon field grows as it rolls down the run-away potential. Near the kink, the slope increases rapidly as the tachyon fluid flows to the kink. In (b),  $\dot{T}$  increases gradually in the bulk region while it increases very rapidly near the kink. If it is evolved further, the slope gets very steep and a caustic is accompanied.

### 3.1 Pure tachyon case ( $\Pi = 0$ )

Let us first consider the pure tachyon case ( $\Pi = 0$ ) in which caustic phenomena have been previously observed in a bit different set-ups [5, 8]. In ref. [5], the authors studied the caustic problem with an arbitrary initial configuration, and treated the tachyon field as collisionless fluid during the evolution. They found that there develop some regions where

the tachyon field becomes multi-valued at a finite time. In ref. [8], the authors studied the tachyon evolution in a very similar way to ours, but with different initial conditions and a potential  $V = \exp(-\alpha T^2)$ . Therefore, it is worthwhile to examine how the caustic phenomenon arises in our set-up if it exists.

For  $\Pi = 0$ , the static solution (3.2) is simplified as

$$T_0(x) = \sqrt{2} \sinh^{-1} \left[ \sqrt{\frac{\mathcal{T}_1^2}{\beta_0^2} - 1} \sin \left( \frac{x}{\sqrt{2}} \right) \right]. \quad (3.6)$$

The proper range of  $\beta_0$  is then given by

$$0 < \beta_0^2 < \mathcal{T}_1^2. \quad (3.7)$$

In the limit of  $\beta_0^2 \rightarrow 0$ , the slopes of the tachyon profile (3.6) at the kink and the anti-kink sites become infinite, and the region between the kink and the anti-kink goes to the closed string vacuum. However, the period of the static tachyon configuration remains at the same constant value  $2\sqrt{2}\pi$ . Therefore, the solution becomes an array of step functions with an infinite height at each site of the kink and the anti-kink [22, 25]. For various values of  $\beta_0$  in the above range, we have performed numerical calculations. We observed that evolutions are more or less similar regardless of the value of  $\beta_0$ . We show numerical results in figure 1 which exhibit a typical evolution behavior.

Beginning with the static configuration and a minimal perturbation, the tachyon field grows as it rolls down the potential. The velocity of the tachyon field  $\dot{T}$  gradually grows everywhere except the fixed nodes where lower dimensional D0/ $\bar{D}0$ -branes are located. The initial static configuration is never physically stable. At late times, we can observe that the velocity near the kink grows faster than in the bulk, and the slope of the tachyon field gets very large. This behavior is very similar to what was observed in ref. [8], so we identify it with the early stage of a caustic formation. When it evolves further, the numerical calculation diverges since the slope becomes too large as in ref. [8].

Due to the caustic behavior at late times, it is not possible to observe the final decay products, such as lower dimensional D-branes and tachyon matter, in the inhomogeneous evolution of the unstable D-brane. Although the main purpose of present work is to investigate the stability of a given kink solution using numerical techniques, let us consider the decay products of our system in an analytic manner. Since we are considering the evolution of an unstable D-brane on a compactified circle, the total energy of the system is finite. The total energy of the initial kink (anti-kink) (3.6) is given by [25],

$$E_{\text{kink}} = \int_{-\frac{\sqrt{2}}{2}\pi}^{\frac{\sqrt{2}}{2}\pi} dx T^{00} = \sqrt{2}\pi \mathcal{T}_1 = \mathcal{T}_0, \quad (3.8)$$

where the energy density  $T^{00}$  is defined in eq. (2.12). The energy of the initial static kink (anti-kink) gives exactly the tension of D0 ( $\bar{D}0$ )-brane for the specific tachyon potential (3.1). Note that the energy does not depend on  $\beta_0$ . In other words, the energy of the expected final decay product D0 ( $\bar{D}0$ ) which corresponds to the kink (anti-kink) in the



thin limit ( $\beta_0 \rightarrow 0$ ) is exactly the same with that of the kink (anti-kink) with an arbitrary  $\beta_0$ . If the story is so, no tachyon matter is produced in principle. For the other kink (anti-kink) solutions in more general runaway-type tachyon potentials [24], the analytic approach becomes more complicated.

For our case, one can expect that the tachyon matter, if it should be produced in the very final stage, would come only from the minimal perturbation applied numerically, but it is a negligible amount. In the numerical evolution, however, such an ideal final stage can never be reached due to the caustic behavior as we described above, so the final decay products are beyond description.

### 3.2 Tachyon with electric flux ( $\Pi \neq 0$ )

In this section, we consider the tachyon evolution with an electric field turned on. It is expected that the fundamental string which connects the lower dimensional D0/ $\bar{D}0$ -branes modulates the tachyon flow and decay.

The electric flux  $\Pi = \beta E$  remains constant during evolution. This is the solution to the gauge field equation as was discussed in section 2. What is remaining is to solve the tachyon field equation, which we shall do numerically with applying  $\Pi$  from a very small value. For  $\Pi \neq 0$ , the static solution (3.2) is valid for

$$\beta_0^2 - \mathcal{T}_1^2 < \Pi^2 < \beta_0^2. \tag{3.9}$$

The value of  $\beta_0$  is not restricted, in principle, once  $\Pi$  is ranged according to the above relation, or vice versa.

#### 3.2.1 Unstable solution

The pure tachyon solution (3.6) is a continuous limit ( $\Pi \rightarrow 0$ ) of the static solution (3.2) with electric field. Therefore, turning on tiny amount of electric flux would not affect the evolution pattern so much, and the result for small  $\Pi$  will be similar to that of the pure tachyon case.

Since we are interested in the tachyon evolution in comparison with the pure tachyon case, first we fix the value of  $\beta_0$  and vary  $\Pi$  in the range (3.9). When  $\Pi$  is very small, we observe from numerical calculations that the tachyon evolves in a very similar way to the pure tachyon case. In figure 2, we show the numerical results for  $\beta_0 = 0.1\mathcal{T}_1$  and  $\Pi = 10^{-3}\beta_0$  (i.e.,  $E_0 = 10^{-3}$ ). The tachyon field grows in time in the bulk, and around the kink/anti-kink at late times it exhibits a similar caustic behavior to what happened in the  $\Pi = 0$  case. When the electric flux is small, the fundamental string cannot properly modulate the tachyon flow to the kink direction. This picture is common for all the values of  $\beta_0$ , and even for  $\beta_0^2 > 1$  which was a prohibited range for the pure tachyon case.

As time elapses, the energy flows from the bulk region to the kink/anti-kink (See figure 3). The energy density (2.12) in Hamiltonian representation is given by

$$\rho = \mathcal{H} = \sqrt{(1 + T'^2)(\Pi^2 + \Pi_T^2 + V^2)}, \tag{3.10}$$

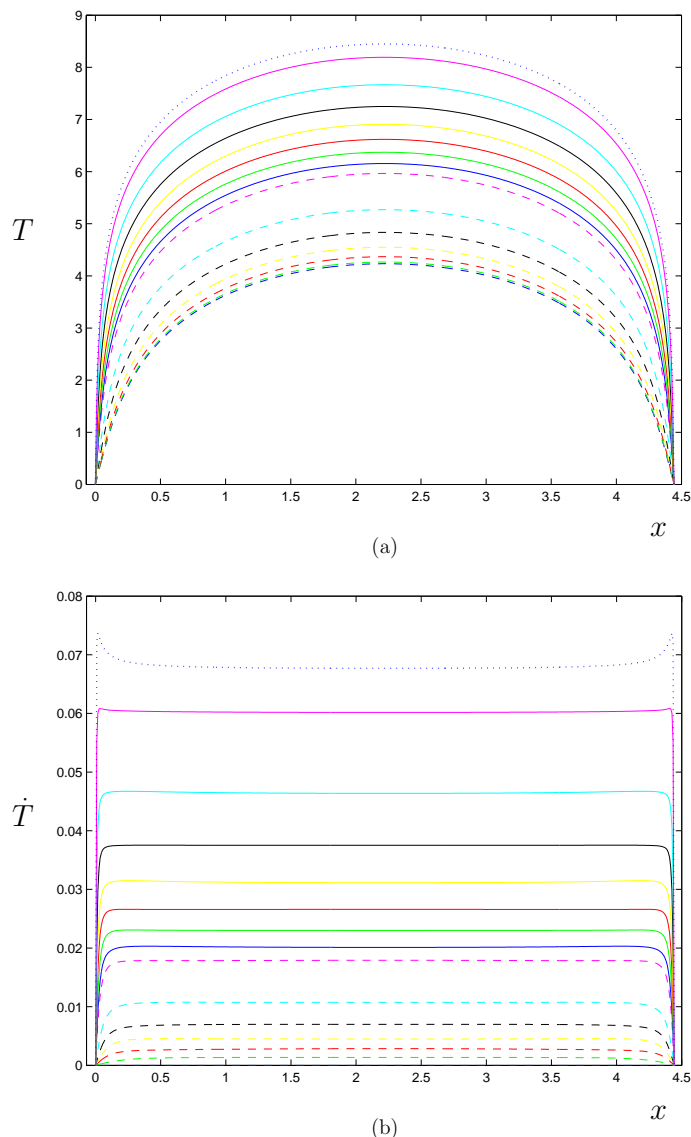


**Figure 2:** Plot of (a)  $T(t, x)$  and (b)  $\dot{T}(t, x)$  for the tachyon-plus-electric field case with  $\beta_0^2 = 10^{-2}T_1^2$  and  $\Pi^2 = 10^{-6}\beta_0^2$ . From the bottom, the lines correspond to  $t = 0, 50, 100, \dots, 300, 310, 320, \dots, 370, 374$ . The overall evolution is very similar to the pure tachyon case, but is lagged a little bit due to the nonvanishing electric flux. This case confronts a caustic in the end.

where the conjugate momentum of the tachyon field  $T$  is

$$\Pi_T = \frac{\partial \mathcal{L}}{\partial \dot{T}} = \beta \dot{T}. \tag{3.11}$$

The plot of  $\rho = T^{00}$  shows that the energy is lumped at the kink/anti-kink, and the corresponding lower dimensional D0/ $\bar{D}0$ -branes become thin due to the nonvanishing momentum flow toward the kink location. As time elapses further, the evolution steps into

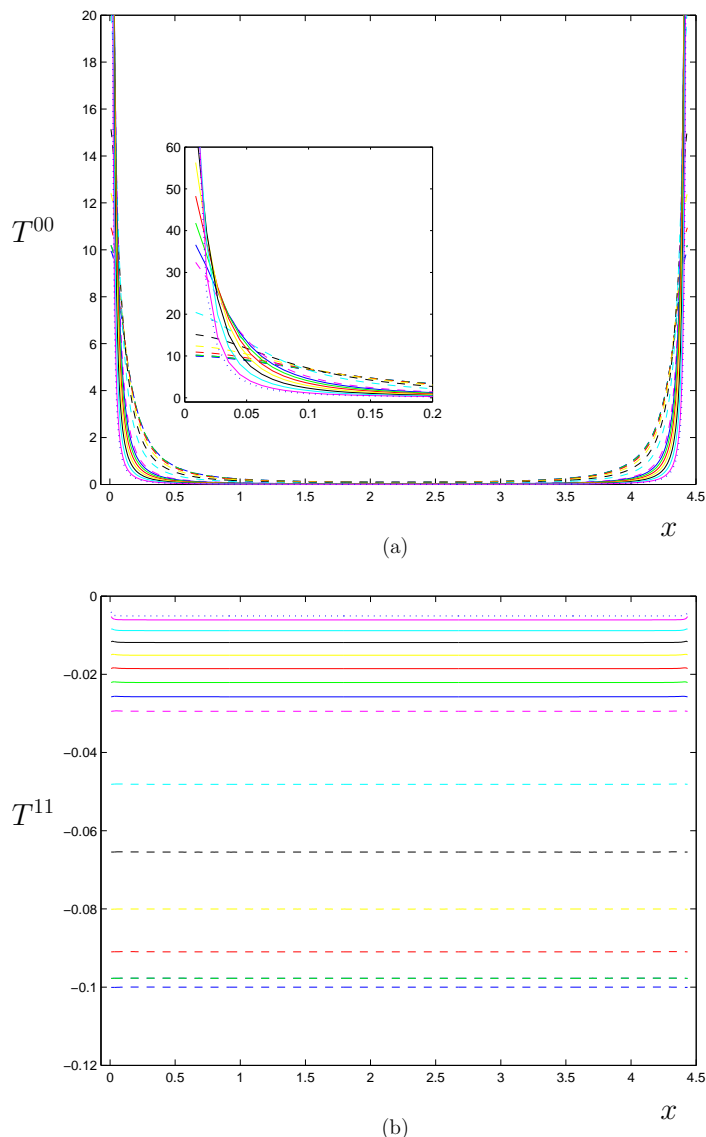


**Figure 3:** Plot of (a) energy density  $T^{00}$  and (b) pressure  $T^{11}$ . As the tachyon evolves, the energy flows from the bulk to the kink and the kink becomes thin. (See the zoom-in plot of the kink region.) The pressure gradually increases to zero from the below.

the initial stage of the caustic formation in a very similar manner discussed in the pure tachyon case, beyond which numerical calculations cannot be performed.

The pressure increases pretty homogeneously to zero from the below as shown in figure 3. The electric field which initially began from a constant value increases more or less homogeneously in the bulk region, but it peaks up at the kink/anti-kink region at late times as shown in figure 4.

Similarly to the case of the pure tachyon in section 3.1, we consider the decay products analytically. Substituting the static solution (3.2) into the energy density relation (2.12),

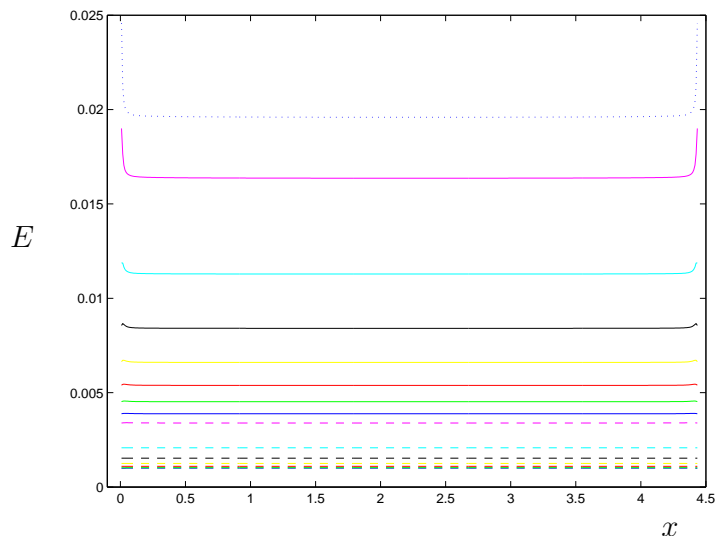


**Figure 4:** Plot of electric field  $E$ .  $E$  grows more or less homogeneously in the bulk region, and peaks near the kink/anti-kink.

we obtain

$$T^{00} = \Pi E_0 + \frac{E_0}{\Pi} \frac{\mathcal{T}_1^2}{1 + \left( \frac{E_0^2 \mathcal{T}_0^2}{\Pi^2 (1 - E_0^2)} - 1 \right) \sin^2 \left( \frac{x}{\xi} \right)}, \quad (3.12)$$

where  $\xi = \sqrt{2}/\sqrt{1 - E_0^2}$ . Integrating over a half period centered at the kink, we obtain the initial total energy generated by the kink [25],

$$E_{\text{kink}} = \int_{-\frac{\xi\pi}{2}}^{\frac{\xi\pi}{2}} dx T^{00} = \frac{\sqrt{2}\pi\Pi^2}{\sqrt{\beta_0^2 - \Pi^2}} + \mathcal{T}_0, \quad (3.13)$$

where  $\beta_0 = \Pi/E_0$  and  $\mathcal{T}_0 = \sqrt{2}\pi\mathcal{T}_1$ . The terms on the right hand side of eq. (3.13) denote the string charge over a half circle and the tension of the D0-brane respectively. The total energy of the kink profile depends on both  $\Pi$  and  $\beta_0$ . The thickness of the kink can also be deduced from the slope of the static solution,

$$T_0(x) \sim \frac{1}{\beta_0} \sqrt{\mathcal{T}_1^2 - (\beta_0^2 - \Pi^2) x}. \quad (3.14)$$

For a given  $\Pi$ , once the tachyon is unstable and experiences changes in its thickness, the evolution would not be in such a way as to follow other static configurations which are described by different  $\beta_0$ 's; the total energy  $E_{\text{kink}}$  is not conserved. Being different from the pure tachyon case in this sense, it is hard to imagine what the final decay products would be. In particular, for our current system in which the electric field  $E$  evolves inhomogeneously near the kink, and which seems to accompany a caustic behavior at late times, it is impossible to discuss analytically the decay products at the final stage.

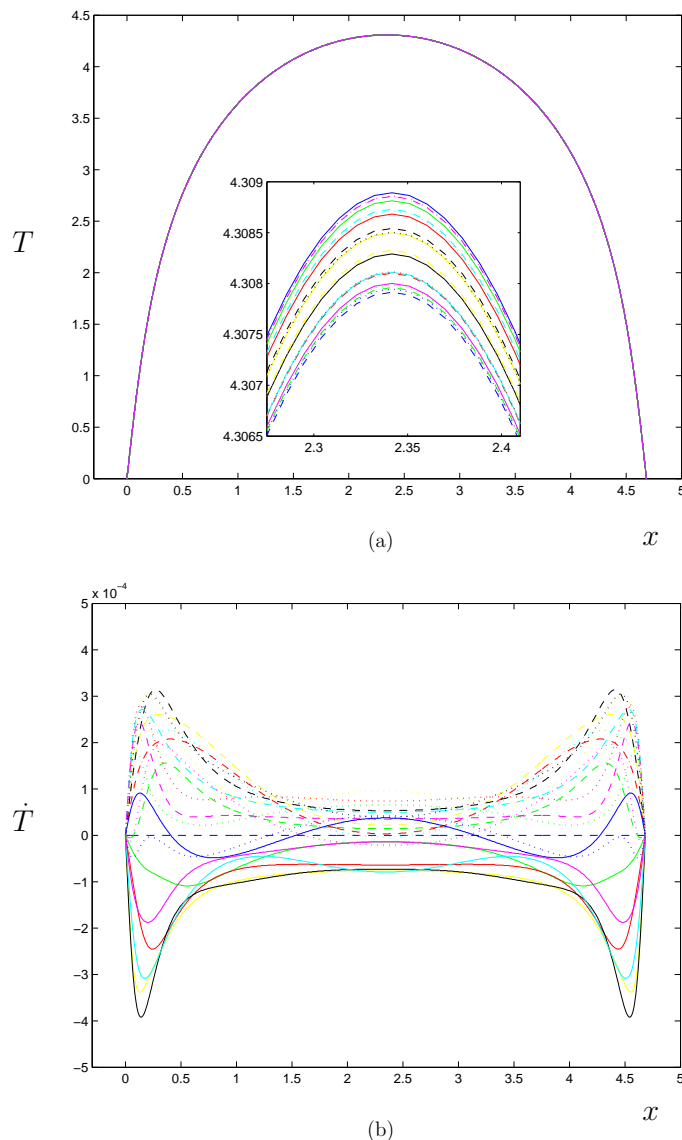


**Figure 5:** Plot of (a)  $T(t, x)$  and (b)  $\dot{T}(t, x)$  for the tachyon-plus-electric field case with  $\beta_0^2 = 10^{-2}\mathcal{T}_1^2$  and  $\Pi^2 = 10^{-1}\beta_0^2$ . The lines correspond to  $t = 0, 30, 60, \dots, 600$ , but are distinguishable only in the zoom-in plot of the top region. The tachyon field is very stable and exhibits only very small oscillations. Although we have not plotted enough time slices, the top part of the tachyon configuration experiences about 20 oscillations till  $t = 600$ . In (b),  $\dot{T}$  also oscillates about zero stably. (Depending on the values of  $\beta_0$  and  $\Pi$ ,  $\dot{T}$  can be less wiggly.)

### 3.2.2 Stable solution

As the value of  $\Pi$  is increased, the electric flux on the fundamental string suppresses more efficiently the tachyon flow toward the kink as well as the tachyon decay in the bulk. Above some critical value of  $\Pi$ , therefore, we expect that the flux completely blocks the tachyon evolution and makes the tachyon stable. The existence of the electric flux (the  $T'^2\Pi^2$  term)

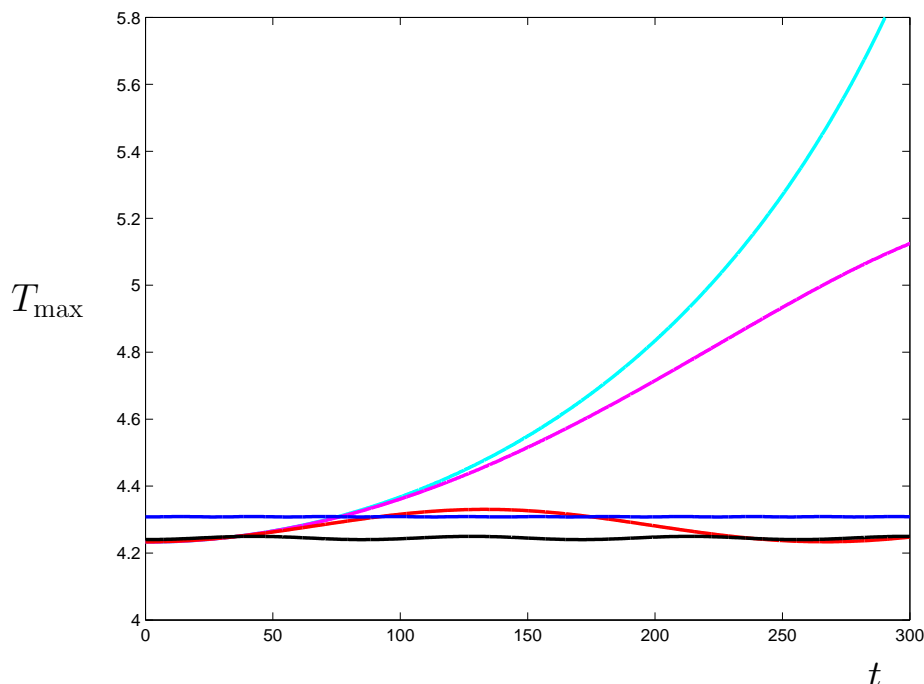


**Figure 6:** Plot of  $T_{\max}$  for  $\beta_0^2 = 10^{-2}\mathcal{T}_1^2$  and  $\Pi^2 = 10^{-6}, 10^{-4}, 10^{-3}, 10^{-2}, 10^{-1}\beta_0^2$ . For subcritical values of  $\Pi$ ,  $T_{\max}$  grows monotonically. For supercritical values of  $\Pi$ ,  $T_{\max}$  becomes stable.

takes parts in the energy density (3.10), which presumably suppress the kinetic portion of the tachyon field for a given system.

From numerical calculations, we observe that the critical value ranges around  $\Pi_c(\beta_0) \sim 0.1\beta_0$ , or less. The numerical coefficient also depends on  $\beta_0$ . In figure 5, we show the numerical results for  $\beta_0 = 0.1\mathcal{T}_1$  and  $\Pi = \sqrt{0.1}\beta_0$ . The tachyon remains very close to the initial static solution with only small oscillations (these are visible in the zoom-in plot only). The velocity  $\dot{T}$  oscillates about zero, which also indicates the stability of tachyon. In figure 6, we plotted the evolution of the maximum value of  $T$  ( $T_{\max}$ ) for several values of  $\Pi$ .

For numerical calculations so far, we have adopted the initial condition (3.4) which implies only a minimal perturbation. Therefore, one may question what would happen if larger perturbations are applied to the stable solutions. The conclusion is that the stable solution remains still stable unless the perturbations are unreasonably large. We have performed numerical calculations with an initial condition,  $\dot{T}(t=0, x) = c_1 \times T(t=0, x)$ , by varying the constant  $c_1$  in a reasonable range ( $|c_1| \ll 1$ ). In figure 7, we plotted the tachyon evolution for  $c_1 = 0.01$  with the same values of the other parameters. The tachyon field remains still stable, although the oscillation amplitude gets larger than that of the minimal perturbation case. For larger  $c_1$ 's, the oscillation amplitudes are larger.

According to our numerical results, the critical electric flux depends on the value of  $\beta_0$ ,  $\Pi_c(\beta_0) \sim 0.1\beta_0$ . For a given  $\beta_0$ , the stability of the kink is guaranteed if  $\Pi \geq \Pi_c$ .

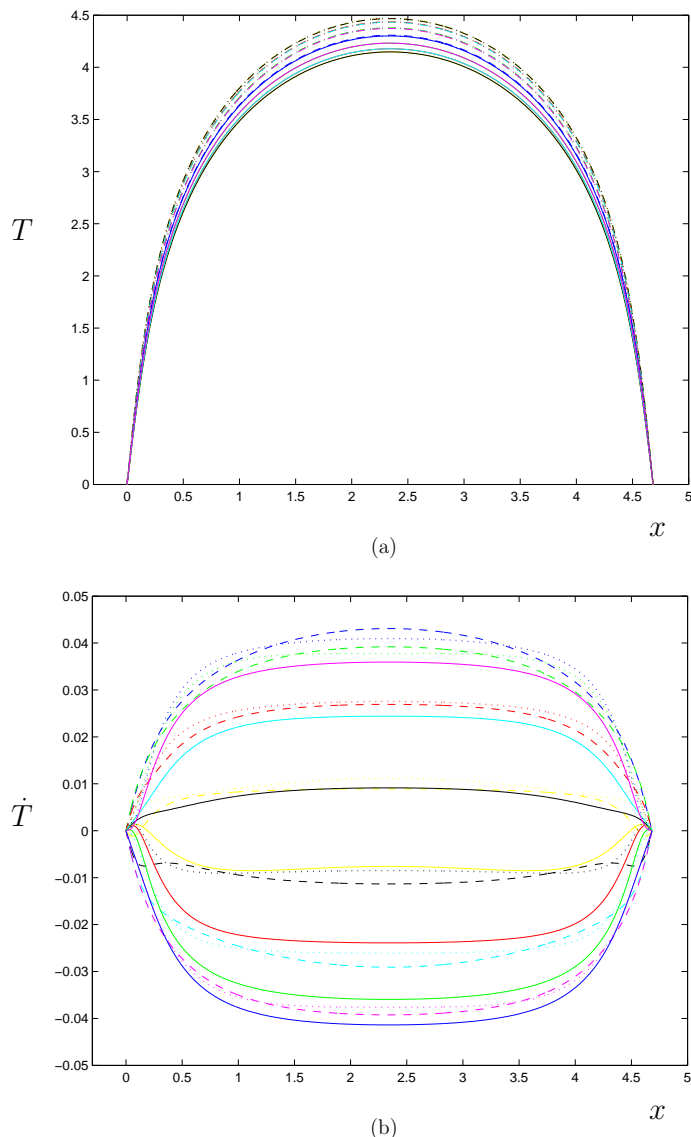


**Figure 7:** Plot of (a)  $T(t, x)$  and (b)  $\dot{T}(t, x)$  for the case of a larger perturbation with an initial velocity  $\dot{T}(0, x) = 0.01T(0, x)$ . The other parameters are the same as in figure 5. The tachyon field oscillates stably about the static solution as in the minimal perturbation case, but with a larger amplitude.

Conversely, for a given  $\Pi$ ,  $\beta_0$  should range as

$$\Pi < \beta_0 \lesssim 10\Pi_c. \tag{3.15}$$

The initial static kink with  $\beta_0$  beyond the above range, is subject to instability. The slope of the kink,  $\sqrt{T_1^2 - (\beta_0^2 - \Pi^2)}/\beta_0$ , also has a constrained range for the stability accordingly; the thickness of the lower dimensional D-brane does so, because it is evaluated roughly as the inverse of the slope.

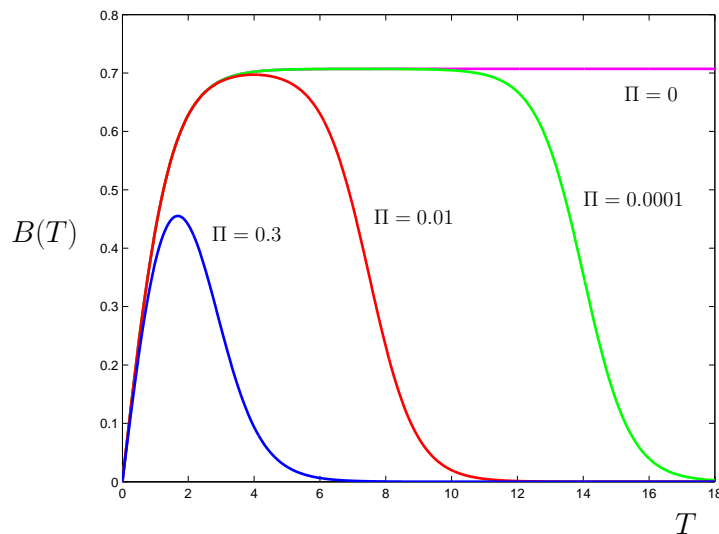


**Figure 8:** Profiles of  $B(T)$  for various  $\Pi$ .

#### 4. Semi-analytic approach

In the previous section, we observed from *numerical* calculations that the static tachyon configuration is stable when the electric flux is sufficiently large. For small or zero electric flux, however, the static configuration is no longer stable; the tachyon rolls down the potential and the caustic forms at the kink. In this section, we would like to capture the stabilization story more conceptually mainly by analyzing the field equation. The analysis will be a bit technical.

The tachyon field equation (2.11) can be arranged as

$$(1 + T'^2)\ddot{T} = (1 - \dot{T}^2) \left[ T'' + (1 + T'^2) B(T) \right] + 2\dot{T}T'\dot{T}' + \dot{T}^2T'^2 B(T), \quad (4.1)$$

where

$$B(T) \equiv \begin{cases} \frac{1}{\sqrt{2}} \tanh\left(\frac{T}{\sqrt{2}}\right), & \text{for } \Pi = 0, \\ \frac{\mathcal{T}_1^2 \operatorname{sech}^2\left(\frac{T}{\sqrt{2}}\right) \tanh\left(\frac{T}{\sqrt{2}}\right)}{\sqrt{2}[\Pi^2 + \mathcal{T}_1^2 \operatorname{sech}^2\left(\frac{T}{\sqrt{2}}\right)]}, & \text{for } \Pi \neq 0. \end{cases} \quad (4.2)$$

It is enough to consider only one patch between the kink ( $x = x_0 = 0$ ) and the anti-kink ( $x = x_1 = \sqrt{2}\pi\beta_0/\sqrt{\beta_0^2 - \Pi^2}$ ) as we did in numerical calculations. Let us call the location of the maximum of  $T$  as  $x_{1/2}$  ( $= x_1/2$ ). Equalizing the square-bracket part in eq. (4.1) to zero corresponds to the static equation. We adopted its solution as the initial configuration. Applying the minimal perturbation discussed in the previous section, we are now interested in how  $\ddot{T}$  behaves in order to check the stability. If its signature remains unchanged,  $T$  will grow/decrease only; the tachyon is unstable. In order to have a stably oscillating tachyon configuration, the signature of  $\ddot{T}$  should keep changing during the evolution. It is sufficient to look up this behavior only in some parts of the patch, so we shall do in the bulk region where the evolution is gentle.



#### 4.1 Pure tachyon case ( $\Pi = 0$ )

Suppose that the tachyon field begins to evolve initially with a tiny positive velocity  $\dot{T}(t = 0, x) > 0$  from the static configuration. The Noether momentum along the  $x$ -direction,

$$P_1 = -\beta\dot{T}T', \tag{4.3}$$

is always negative (positive) in the region  $0 < x < x_{1/2}$  ( $x_{1/2} < x < x_1$ ). Therefore, the energy density flows to the kink (anti-kink) accordingly, and there grows the slope of  $T$  as well. And the corresponding term,  $2\dot{T}T'\dot{T}' + \dot{T}^2T'^2B(T)$ , in eq. (4.1) is always positive.

The remaining factor in eq. (4.1) in determining the change in  $\ddot{T}$  is now the square-bracket part

$$\left[ T'' + \frac{1 + T'^2}{\sqrt{2}} \tanh\left(\frac{T}{\sqrt{2}}\right) \right]. \tag{4.4}$$

Initially this is zero since we adopted the static solution as the initial condition. As time elapses, we observed from numerical calculations that the curvature  $T''$  remained more or less unchanged in negative in the bulk while  $T$  grows. Therefore, the above term (4.4) remains positive since its second term is a growing function of  $T$ .

As a whole, all the terms on the right hand side of eq. (4.1) remain positive, which keeps  $\ddot{T}$  positive; the tachyon is unstable to grow in the bulk region and to form caustic about the kink and the anti-kink.

The tachyon velocity  $\dot{T}$  does not exceed one in the middle of the bulk region, which can be understood from the following. The slope  $T'$  and the curvature  $T''$  in this region is relatively small, so we can approximate the tachyon field equation to a homogeneous one

$$\ddot{T} = \frac{1}{\sqrt{2}}(1 - \dot{T}^2) \tanh\left(\frac{T}{\sqrt{2}}\right). \tag{4.5}$$

The solutions to this equation are given by [41],

$$T(t) = \begin{cases} \sqrt{2} \sinh^{-1} \left[ A_c \cosh\left(\frac{t}{\sqrt{2}}\right) \right] \\ \sqrt{2} \sinh^{-1} \left[ A_e \exp\left(\frac{t}{\sqrt{2}}\right) \right] \\ \sqrt{2} \sinh^{-1} \left[ A_s \sinh\left(\frac{t}{\sqrt{2}}\right) \right] \end{cases}, \tag{4.6}$$

where the constants  $A_c$  and  $A_s$  depend on the initial energy density and are less than  $\sqrt{2}$  while  $A_e$  is an arbitrary constant. Then  $|\dot{T}|$  remains less than one for all of the solutions in eq. (4.6) and approaches one at infinity.

#### 4.2 Tachyon with electric flux ( $\Pi \neq 0$ )

If the electric flux is turned on, the only difference in the field equation (4.1) is  $B(T)$  defined in eq. (4.2). Unlike the pure tachyon case,  $B(T)$  is now a bump-like function of  $T$  of which maximum is at

$$T = T_{\max} \equiv \sqrt{2} \operatorname{sech}^{-1} \left[ \frac{\sqrt{(9\Pi^4 + 8\Pi^2 T_1^2)^{1/2} - 3\Pi^2}}{\sqrt{2T_1^2}} \right]. \tag{4.7}$$

We plotted  $B(T)$  for several values of  $\Pi$  in figure 8.

The square-bracket part

$$\left[ T'' + (1 + T'^2)B(T) \right] \quad (4.8)$$

which is initially set to zero can become negative if  $T$  is on the descending region of  $B(T)$ . Then, it can possibly happen that the acceleration  $\ddot{T}$  becomes negative. If the decelerating state ( $\ddot{T} < 0$ ) maintains, the velocity will change its signature and become negative,  $\dot{T} < 0$ . Then  $T$  decreases and rolls back up the right hill of  $B(T)$ . The square-bracket (4.8),  $\ddot{T}$ , and  $\dot{T}$  evolve in an opposite way to that during descending.  $T$  will eventually change its direction in the end. This process keeps  $T$  oscillating about a certain configuration, and thus the tachyon becomes stable. The stabilization in this way is more probable for larger  $\Pi$  since the maximum of  $B(T)$  is lower; a certain amount of electric flux is required in order to halt the tachyon rolling down the potential and the flow to the kink. This agrees with our numerical results obtained in the previous section.

### 4.3 Caustic formation revisited

Before we close this section, let us consider the tachyon flow and the caustic formation in the kink region. The quantity  $-X$  in eq. (2.6) should be positive for a physical system. However, when a caustic formation is accompanied ( $\Pi < \Pi_c$ ), it was observed from numerical calculations that the value of  $-X$  at the adjacent position to the kink falls to zero and then becomes negative. This behavior of  $-X$  occurs just before the numerical calculation diverges due to the large slope of  $T$ . This is very similar to the pure tachyon result in ref. [8] where the authors used a different tachyon potential.

Following the techniques in refs. [5, 8], we can estimate the critical time at which the fluid element at the adjacent position reaches the kink. Once  $-X$  becomes zero at a position, assume that the tachyon evolution is constrained by

$$-X = 1 - \dot{T}^2 + T'^2 - E^2 = \frac{\mathcal{T}_1^2 V^2}{\Pi^2 + \mathcal{T}_1^2 V^2} (1 - \dot{T}^2 + T'^2) = 0, \quad (4.9)$$

where we used eq. (2.10) in the second step. As  $\mathcal{T}_1^2 V^2 / (\Pi^2 + \mathcal{T}_1^2 V^2)$  is nonzero, for  $\Pi < \Pi_c$ , the system is governed by the equation

$$1 - \dot{T}^2 + T'^2 = 0, \quad (4.10)$$

which is exactly the same one for the pure tachyon case. Then the results in refs. [5, 8] are applied exactly in the same way as follows.

This first order partial differential equation was solved analytically by the method of characteristics [5]. We introduce a parameter  $q$  which satisfies  $x(q, t_i) = q$ ,  $t(q, t_i) = 0$ , and  $T(q, t_i) = T_i(q)$  at the initial moment  $t_i$  (we set  $t_i = 0$ ). Then the solutions to the equation (4.10) are

$$x_c(q, t) = q - \frac{T_{i,q}}{\sqrt{1 + T_{i,q}^2}} t, \quad (4.11)$$

$$T(q, t) = T_i(q) + \frac{t}{\sqrt{1 + T_{i,q}^2}}, \quad (4.12)$$

where  $T_{i,q} \equiv \partial T_i / \partial q$  and  $x_c(q, t)$  is the characteristic curve of  $q$  at  $t$ . After a finite time  $t = q\sqrt{1 + T_{i,q}^2}/T_{i,q}$ ,  $x_c$  will cross  $x = 0$  with a nonzero value of tachyon field,  $T(q, t) = T_i(q) + q/T_{i,q}$ . Finally the tachyon field becomes multi-valued there, and its slope diverges [8]. The caustic forms firstly at the minimum of  $t = q\sqrt{1 + T_{i,q}^2}/T_{i,q}$ .

## 5. Conclusions

We investigated the numerical evolution of an inhomogeneous D1-brane with a string charge density. We considered a DBI-type action which contains a tachyon field  $T$  with a run-away potential  $V = 1/\cosh(T/\sqrt{2})$  and a gauge field  $A_1$  in a flat (1+1) dimensional spacetime. The target space that we considered is a compactified circle  $S^1$  with a fixed radius. The tachyon field presents an inhomogeneous kink and anti-kink array on the circle. The fundamental string which we considered induces an electric field  $E$  on the D1-brane. The electric flux  $\Pi$  (the string charge density) is solved to be constant while the electric field is let to vary both in time and in space.

There exists a static solution when the electric field is constant,  $E = E_0$  [23, 25]. We focus our interest on the case of  $0 \leq E_0 < 1$  for which the tachyon profiles represent a kink-anti-kink array. For the pure tachyon case ( $E_0 = 0$ ), it had been studied in refs. [5, 8] that the tachyon field is unstable to form a caustic at the location of the kink, or the anti-kink; the tachyon field becomes double-valued at a finite time, and thus the lower dimensional D-brane becomes thin.

For the initial configuration in evolving the tachyon field, we adopt the static solution of which configuration is determined by two parameters, the electric flux  $\Pi$  and the electric field  $E_0$  (or  $\beta_0 = \Pi/E_0$ ). The compactification radius is then fixed to  $\sqrt{2}/\sqrt{1 - E_0^2}$ . The electric flux  $\Pi$  remains constant during the evolution as a solution to the gauge field equation, while  $E$  ( $\beta$ ) is allowed change. Applying a minimal perturbation on the initial configuration, we evolved the tachyon field.

When the string charge density  $\Pi$  is zero or sufficiently small, the tachyon is unstable regardless of the initial pressure of the tachyon kink,  $-\beta_0$ .  $T$  rolls down the potential  $V$ , and its slope gets large at the kink and the anti-kink. Although it is never possible to reach numerically the infinite-slope state, we expect that the tachyon configuration approaches the situation of caustic formation in a similar way discussed in ref. [8]. According to the Sen's proposal in [1], the final state can be interpreted as a thin D0- $\bar{D}0$  pair located diametrically opposite points on the circle [34–36].

When  $\Pi$  is sufficiently large, the tachyon becomes stabilized. The initial static solution remains stable even when larger perturbations are applied. The fundamental string connecting D0- and  $\bar{D}0$ -branes modulates the tachyon flow and provides the stability. The stabilization is achieved when the electric flux is larger than some critical value  $\Pi > \Pi_c$  where  $\Pi_c$  is a function of the initial  $\beta_0$ , and numerically it is  $\Pi_c \sim 0.1\beta_0$ . The stable kink with  $\Pi > \Pi_c$  is identified as the lower dimensional stable thick D-brane with thickness  $\sim \beta_0/\sqrt{\mathcal{T}_1 - \beta_0^2}$ .

It is not sufficient, however, to fully discuss the stability of the resulting thick D0- $\bar{D}0$  pair with our limited boundary and initial conditions. To clarify the properties of the

system, one needs more investigations with various boundary and initial conditions. For example, if one imposes a deformed initial velocity of the tachyon and an appropriate boundary condition, one would be able to observe pair annihilation of kink and anti-kink which is related to the instability due to D0 and  $\bar{D}0$  charges.

Another example will be to consider varying radius of  $S^1$  in time, or to consider the evolution on  $R_1$ . In this case, the period of the tachyon kink which was initially set to  $2\sqrt{2}\pi/\sqrt{1-E_0^2}$ , may change in time. One possible way of evolution is to track the successive static solutions of different periods. The electric field then evolves homogeneously.

Our numerical study in this work was the first step to investigating the instability of the tachyon-plus-electric flux system, with the conditions which preserve involved symmetries maximally. In the future, we hope our work is extended to other various directions.

## Acknowledgments

We are grateful to Gary Felder, Gungwon Kang, Chanju Kim, Yoonbai Kim, and Piljin Yi for very useful discussions. This work was supported by the BK 21 project of the Ministry of Education and Human Resources Development, Korea (I.C. and C.O.L.), by the Astrophysical Research Center for the Structure and Evolution of the Cosmos (ARCSEC) and the grant No. R01-2006-000-10965-0 from the Basic Research Program of the Korea Science & Engineering Foundation (I.C.), and by the Science Research Center Program of the Korea Science and Engineering Foundation through the Center for Quantum Spacetime (CQUeST) of Sogang University with grant number R11-2005-021 (O.K.).

## References

- [1] A. Sen, *Time evolution in open string theory*, *JHEP* **10** (2002) 003 [[hep-th/0207105](#)].
- [2] F. Larsen, A. Naqvi and S. Terashima, *Rolling tachyons and decaying branes*, *JHEP* **02** (2003) 039 [[hep-th/0212248](#)].
- [3] S.-J. Rey and S. Sugimoto, *Rolling of modulated tachyon with gauge flux and emergent fundamental string*, *Phys. Rev. D* **68** (2003) 026003 [[hep-th/0303133](#)].
- [4] A. Ishida and S. Uehara, *Rolling down to D-brane and tachyon matter*, *JHEP* **02** (2003) 050 [[hep-th/0301179](#)].
- [5] G.N. Felder, L. Kofman and A. Starobinsky, *Caustics in tachyon matter and other Born-Infeld scalars*, *JHEP* **09** (2002) 026 [[hep-th/0208019](#)].
- [6] S. Mukohyama, *Inhomogeneous tachyon decay, light-cone structure and D-brane network problem in tachyon cosmology*, *Phys. Rev. D* **66** (2002) 123512 [[hep-th/0208094](#)].
- [7] M. Berkooz, B. Craps, D. Kutasov and G. Rajesh, *Comments on cosmological singularities in string theory*, *JHEP* **03** (2003) 031 [[hep-th/0212215](#)].
- [8] J.M. Cline and H. Firouzjahi, *Real-time D-brane condensation*, *Phys. Lett. B* **564** (2003) 255 [[hep-th/0301101](#)].
- [9] G.N. Felder and L. Kofman, *Inhomogeneous fragmentation of the rolling tachyon*, *Phys. Rev. D* **70** (2004) 046004 [[hep-th/0403073](#)].

- [10] N. Barnaby and J.M. Cline, *Creating the universe from brane-antibrane annihilation*, *Phys. Rev. D* **70** (2004) 023506 [[hep-th/0403223](#)].
- [11] N. Barnaby, *Caustic formation in tachyon effective field theories*, *JHEP* **07** (2004) 025 [[hep-th/0406120](#)].
- [12] K.L. Panigrahi, *D-brane dynamics in Dp-brane background*, *Phys. Lett. B* **601** (2004) 64 [[hep-th/0407134](#)].
- [13] O. Saremi, L. Kofman and A.W. Peet, *Folding branes*, *Phys. Rev. D* **71** (2005) 126004 [[hep-th/0409092](#)].
- [14] F. Canfora, *A note on tachyon dynamics*, *Phys. Lett. B* **625** (2005) 277 [[gr-qc/0508082](#)].
- [15] O-K. Kwon and C.O. Lee, *Late time behaviors of an inhomogeneous rolling tachyon*, *Phys. Rev. D* **73** (2006) 126001 [[hep-th/0601236](#)].
- [16] A. Sen, *Rolling tachyon*, *JHEP* **04** (2002) 048 [[hep-th/0203211](#)].
- [17] A. Sen, *Tachyon matter*, *JHEP* **07** (2002) 065 [[hep-th/0203265](#)].
- [18] A. Sen, *Field theory of tachyon matter*, *Mod. Phys. Lett. A* **17** (2002) 1797 [[hep-th/0204143](#)].
- [19] S. Sugimoto and S. Terashima, *Tachyon matter in boundary string field theory*, *JHEP* **07** (2002) 025 [[hep-th/0205085](#)];  
J.A. Minahan, *Rolling the tachyon in super BSFT*, *JHEP* **07** (2002) 030 [[hep-th/0205098](#)];  
A. Ishida, Y. Kim and S. Kouwn, *Homogeneous rolling tachyons in boundary string field theory*, *Phys. Lett. B* **638** (2006) 265 [[hep-th/0601208](#)].
- [20] G. Gibbons, K. Hashimoto and P. Yi, *Tachyon condensates, Carrollian contraction of Lorentz group and fundamental strings*, *JHEP* **09** (2002) 061 [[hep-th/0209034](#)].
- [21] C. Kim, H.B. Kim, Y. Kim and O-K. Kwon, *Electromagnetic string fluid in rolling tachyon*, *JHEP* **03** (2003) 008 [[hep-th/0301076](#)].
- [22] A. Sen, *Dirac-Born-Infeld action on the tachyon kink and vortex*, *Phys. Rev. D* **68** (2003) 066008 [[hep-th/0303057](#)].
- [23] N. Lambert, H. Liu and J.M. Maldacena, *Closed strings from decaying D-branes*, *JHEP* **03** (2007) 014 [[hep-th/0303139](#)].
- [24] P. Brax, J. Mourad and D.A. Steer, *Tachyon kinks on non BPS D-branes*, *Phys. Lett. B* **575** (2003) 115 [[hep-th/0304197](#)];  
E.J. Copeland, P.M. Saffin and D.A. Steer, *Singular tachyon kinks from regular profiles*, *Phys. Rev. D* **68** (2003) 065013 [[hep-th/0306294](#)];  
D. Bazeia, R. Menezes and J.G. Ramos, *Regular and periodic tachyon kinks*, *Mod. Phys. Lett. A* **20** (2005) 467 [[hep-th/0401195](#)].
- [25] C. Kim, Y. Kim and C.O. Lee, *Tachyon kinks*, *JHEP* **05** (2003) 020 [[hep-th/0304180](#)].  
C. Kim, Y. Kim, O-K. Kwon and C.O. Lee, *Tachyon kinks on unstable Dp-branes*, *JHEP* **11** (2003) 034 [[hep-th/0305092](#)].
- [26] V. Afonso, D. Bazeia and F.A. Brito, *Deforming tachyon kinks and tachyon potentials*, *JHEP* **08** (2006) 073 [[hep-th/0603230](#)].
- [27] C. Kim, Y. Kim, O-K. Kwon and H.-U. Yee, *Tachyon kinks in boundary string field theory*, *JHEP* **03** (2006) 086 [[hep-th/0601206](#)].

- [28] Y. Kim, B. Kyae and J. Lee, *Global and local D-vortices*, *JHEP* **10** (2005) 002 [[hep-th/0508027](#)];  
I. Cho, Y. Kim and B. Kyae, *Df-strings from D3 D3-bar as cosmic strings*, *JHEP* **04** (2006) 012 [[hep-th/0510218](#)].
- [29] G.W. Gibbons, K. Hori and P. Yi, *String fluid from unstable D-branes*, *Nucl. Phys.* **B 596** (2001) 136 [[hep-th/0009061](#)].
- [30] O-K. Kwon and P. Yi, *String fluid, tachyon matter and domain walls*, *JHEP* **09** (2003) 003 [[hep-th/0305229](#)].
- [31] H.-U. Yee and P. Yi, *Open/closed duality, unstable D-branes and coarse-grained closed strings*, *Nucl. Phys.* **B 686** (2004) 31 [[hep-th/0402027](#)].
- [32] P. Yi, *Membranes from five-branes and fundamental strings from Dp-branes*, *Nucl. Phys.* **B 550** (1999) 214 [[hep-th/9901159](#)].
- [33] O. Bergman, K. Hori and P. Yi, *Confinement on the brane*, *Nucl. Phys.* **B 580** (2000) 289 [[hep-th/0002223](#)].
- [34] A. Sen, *SO(32) spinors of type-I and other solitons on brane-antibrane pair*, *JHEP* **09** (1998) 023 [[hep-th/9808141](#)].
- [35] A. Sen, *BPS D-branes on non-supersymmetric cycles*, *JHEP* **12** (1998) 021 [[hep-th/9812031](#)].
- [36] A. Sen, *Moduli space of unstable D-branes on a circle of critical radius*, *JHEP* **03** (2004) 070 [[hep-th/0312003](#)].
- [37] M.R. Garousi, *Tachyon couplings on non-BPS D-branes and Dirac-Born-Infeld action*, *Nucl. Phys.* **B 584** (2000) 284 [[hep-th/0003122](#)].
- [38] E.A. Bergshoeff, M. de Roo, T.C. de Wit, E. Eyras and S. Panda, *T-duality and actions for non-BPS D-branes*, *JHEP* **05** (2000) 009 [[hep-th/0003221](#)].
- [39] J. Kluson, *Proposal for non-BPS D-brane action*, *Phys. Rev.* **D 62** (2000) 126003 [[hep-th/0004106](#)].
- [40] A. Sen, *Open-closed duality at tree level*, *Phys. Rev. Lett.* **91** (2003) 181601 [[hep-th/0306137](#)].
- [41] Y. Kim and O-K. Kwon, *Exact rolling tachyon in noncommutative field theory*, *Mod. Phys. Lett.* **A 21** (2006) 421 [[hep-th/0501016](#)].